ADVANCES IN ATMOSPHERIC SCIENCES, 2023

• **Original Paper** •

The Climate Response to Global Forest Area Changes under Different Warming Scenarios in China

Ying HUANG[1], Anning HUANG*[1,2], and Jie TAN[1,3]

[1]*School of Atmospheric Sciences*, *Nanjing University*, *Nanjing* 210023, *China*

[2]*Frontiers Science Center for Critical Earth Material Cycling*, *Nanjing University*, *Nanjing* 210023, *China*

[3]*Glarun Technology Co.*, *Ltd.*, *Nanjing* 211106, *China*

(Received 19 September 2022; revised 3 November 2022; accepted 21 November 2022)

ABSTRACT

Human activities have notably affected the Earth's climate through greenhouse gases (GHG), aerosol, and land use/land cover change (LULCC). To investigate the impact of forest changes on regional climate under different shared socioeconomic pathways (SSPs), changes in surface air temperature and precipitation over China under low and medium/high radiative forcing scenarios from 2021 to 2099 are analyzed using multimodel climate simulations from the Coupled Model Intercomparison Project Phase 6 (CMIP6). Results show that the climate responses to forest changes are more significant under the low radiative forcing scenario. Deforestation would increase the mean, interannual variability, and the trend of surface air temperature under the low radiative forcing scenario, but it would decrease those indices under the medium/high radiative forcing scenario. The changes in temperature show significant spatial heterogeneity. For precipitation, under the low radiative forcing scenario, deforestation would lead to a significant increase in northern China and a significant decrease in southern China, and the effects are persistent in the near term (2021–40), middle term (2041–70), and long term (2071–99). In contrast, under the medium/high radiative forcing scenario, precipitation increases in the near term and long term over most parts of China, but it decreases in the middle term, especially in southern, northern, and northeast China. The magnitude of precipitation response to deforestation remains comparatively small.

Key words: land use/land cover change, deforestation, radiative forcing scenario, regional climate

Citation: Huang, Y., A. N. Huang, and J. Tan, 2023: The climate response to global forest area changes under different warming scenarios in China. *Adv. Atmos. Sci.*, https://doi.org/10.1007/s00376-022-2230-z.

Article Highlights:

- The temperature and precipitation changes in China due to deforestation have different responses under different climate warming backgrounds, and the responses are more significant under the low radiative forcing scenario.
- Deforestation would lead to an increase in the annual mean surface air temperature and its interannual variability and trend in all seasons under the low radiative forcing scenario, and these changes show significant regional differences.
- Deforestation would lead to a significant increase (decrease) in precipitation in northern (southern) China under the low radiative forcing scenario. In contrast, the responses of temperature and precipitation changes are uncertain under the medium/high radiative forcing scenario.

1. Introduction

The IPCC has indicated that greenhouse gases (GHG), aerosol, and large-scale land use/land cover change (LULCC) are important anthropogenic activities that have induced historical climate change over the past century and are expected to continue to affect future climate (IPCC, 2021). Increasing concentrations of greenhouse gases warm the global atmosphere, intensify the hydrological cycle, and increase precipitation in many regions, whereas LULCC affects land–atmosphere interactions by altering biophysical processes, which in turn affect regional and global climate (Held and Soden, 2006; Hurtt et al., 2006; Pitman et al., 2009, 2011; Yang et al., 2009; Pielke et al., 2011; Wan et al., 2014; Xu et al., 2015, 2017; Zhu et al., 2018; Huang et al., 2020). While previous modeling and observational studies have shown that the global averaged LULCC impacts on temperature and rainfall are negligible, the regional impacts can be of similar magnitude to CO_2-induced changes, or even stronger and more statistically significant than the CO_2 warming effects (Foley et al., 2005; Arora and Montenegro,

* Corresponding author: Anning HUANG
Email: anhuang@nju.edu.cn

© Institute of Atmospheric Physics/Chinese Academy of Sciences, and Science Press and Springer-Verlag GmbH Germany, part of Springer Nature 2023

2011; Lawrence et al., 2012; Pitman et al., 2012; Shao and Zeng, 2012; Brovkin et al., 2013; Chen et al., 2015; Hua et al., 2015; Yuan and Zhai, 2022).

Afforestation is one of the most important human activities causing land use/land cover changes and is an important approach to mitigate global warming. Forests store large amounts of carbon, about 1.5 times that stored in the atmosphere (Dixon et al., 1994). The International Union of Forest Research Organizations (IUFRO) report (FAO, 2009) indicates that the carbon dioxide release from historical deforestation accounts for almost one fifth of the increasing CO_2 in the atmosphere. Previous studies have shown that forests dampen or amplify anthropogenic climate change through complex and nonlinear forest–atmosphere interactions (Bonan, 2008; Lee et al., 2011; Alkama and Cescatti, 2016). Forests induce important climate forcings and feedbacks. For instance, forests have a lower albedo than other land cover types, which contributes to amplifying local warming through decreasing surface albedo and increasing shortwave radiation (the radiative effect). Conversely, forests promote the hydrologic cycle through evapotranspiration, which causes local cooling (the nonradiative effect) (Pitman et al., 2009; Davin and de Noblet-Ducoudré, 2010; Mao et al., 2011). Li et al. (2015) reported that tropical forests had a strong cooling effect throughout the year, temperate forests showed moderate cooling (warming) in summer (winter) with a net cooling effect annually, and boreal forests showed strong warming in winter and moderate cooling in summer with a net warming effect annually. Such forest-induced spatiotemporal differences in temperature responses result from the divergent changes of the radiative effect (albedo) and the nonradiative effect (evapotranspiration) in different regions. In general, the radiative effect of forests tends to dominate at high latitudes while the nonradiative effect is more important over the tropics. The radiative and nonradiative effects tend to counterbalance each other in the temperate forests (Perugini et al., 2017).

Evidence from both observations (Yang et al., 2010; Duveiller et al., 2018; Ge et al., 2019) and climate models (Davin and de Noblet-Ducoudré, 2010; Lorenz et al., 2016; Boysen et al., 2020) has shown that the biophysical impact of deforestation warms the tropics and cools the boreal regions, while the response to deforestation in the midlatitudes is uncertain. Li et al. (2016) suggested that the latitudinal pattern of temperature response depends nonlinearly on the spatial extent and the intensity of deforestation. Temperature change due to global deforestation is greatly amplified in temperate and boreal regions but is dampened in tropical regions. These divergent temperature patterns reveal the importance of the background climate in modifying the deforestation impact. Deforestation can impact precipitation through biophysical processes, which lead to decreased annual average precipitation, reduced heavy precipitation frequency/intensity, and shortened duration of rainy seasons over the deforested areas (Luo et al., 2022).

To address growing environmental concerns and deal with global warming, China has developed the Three-North Shelterbelt Development Program, the Natural Forest Conservation Program, and the Grain for Green Program, and plans to expand afforestation in the near future (Liu et al., 2008; Fu et al., 2017; Bryan et al., 2018). Therefore, investigation of the overall climate impact of global forest changes over China is one strategy demand for China's afforestation policies. Due to the uncertain effects of forest changes on regional temperature and precipitation through biophysical and biochemical processes, the regional impacts of LULCC depend not only on the background climate but also on the background climate change (Pielke and Avissar, 1990; Taylor et al., 2002; Sun and Mu, 2013; Hua et al., 2017). Pitman et al. (2011) noted that increasing greenhouse gases have caused changes in snow and rainfall, which affect the snow–albedo feedback and the water supply, which in turn limits evaporation. The above changes largely control the net impact of LULCC on regional climate. The LULCC-induced radiative forcing (RF) is different under different background climates with GHG concentrations in 1850 and in the present age, thus leading to different temperature and precipitation responses to LULCC (Hua and Chen, 2013; Hu et al., 2018). Will the regional impact of afforestation be different in China during global warming, and which part has the strongest effects? These effects remain poorly understood at present and require further investigation.

Along with human social activities and economic development, will future increasing greenhouse gas emissions and expanding LULCC result in increased precipitation and temperature, and more significant regional climate effects? These require further exploration. Therefore, CMIP6 has endorsed the Land Use Model Intercomparison Project (LUMIP). The LUMIP model experiments have been developed in consultation with several existing model intercomparison activities and research programs that focus on the biogeophysical impact of land use on climate. The simulations can be used to quantify the historic impact of land use and explore the potential for future land management decisions to aid in mitigation of climate change (Lawrence et al., 2016). The impact of the different land use scenarios on the future climate, especially on the regional climate, has implications for understanding the role of land use and land management in regional climate mitigation (Hong et al., 2022). In this study, we aim to investigate the impact of changes in forest area under different emissions scenarios on regional climate over China by using LUMIP multimodel climate simulations. The analyses of the future global deforestation experiments could advance our understanding of deforestation-induced climate changes, and provide new guidance to afforestation strategies and climate change mitigation policy.

2. Data and method

2.1. *Data*

In this study, we used monthly precipitation and surface

air temperature (SAT) data from five climate models that participate in the Coupled Model Intercomparison Project Phase 6 (CMIP6) (Table 1), including historical runs, Scenario Model Intercomparison Project (ScenarioMIP), and Land-Use Model Intercomparison Project (LUMIP). For ScenarioMIP, we selected two future scenarios: SSP1-2.6 and SSP3-7.0 (global radiative forcing of 2.6 W m^{-2} and 7.0 W m^{-2} by 2100, respectively) from 2015 to 2100. For LUMIP, the two future land-use policy sensitivity experiments (i.e., SSP370-SSP126Lu and SSP126-SSP370Lu) from 2015 to 2099 were used (Table 2).

LUMIP experiments are derivatives of ScenarioMIP (SSP3-7.0 and SSP1-2.6) simulations. This particular set of simulations was selected because the projected land-use trends in SSP3-7.0 and SSP1-2.6 diverge strongly, with SSP3-7.0 representing a reasonably strong deforestation scenario (global forest area decreases from 38 million km^2 to 33 million km^2 during 2015–2100) and SSP1-2.6 including significant afforestation (global forest area increases from 37 million km^2 to 43 million km^2 during 2015–2100). Within the LUMIP framework, these simulations design concentration-driven variants of ScenarioMIP SSP3-7.0 and SSP1-2.6, but each uses the land-use scenario from the other. The SSP370-SSP126Lu experiment runs with all forcings identical to SSP3-7.0, except that the land use is taken from SSP1-2.6. In contrast, the SSP126-SSP370Lu experiments use all forcing from SSP1-2.6, except for the land use from SSP3-7.0. The LUMIP experiments are described in detail in Lawrence et al. (2016).

2.2. *Division of subregions*

To examine the regional differences in impacts, China is divided into ten subregions: NE (northeast China), NC (north China), IM (Inner Mongolia), CC (central China), EC (east China), SC (south China), SW (southwest China), NW (northwest China), XZ (Xizang), and XJ (Xinjiang) according to administrative boundaries as well as geographical and societal conditions (Fig. 1).

2.3. *Quantification of the regional impact of deforestation*

We used SSP126-SSP370Lu minus SSP1-2.6, and SSP3-7.0 minus SSP370-SSP126Lu to represent the response of deforestation under the low and medium/high radiative forcing scenarios, respectively. We compared the LULCC effects in two scenarios to examine the extent to which the impact of deforestation differs at different levels of climate change (Lawrence et al., 2016; Hua et al., 2021; Wang et al., 2021).

Given the different horizontal resolutions across the models, all model outputs were bilinearly interpolated to the horizontal resolution of 0.5°×0.5°, and the ensemble mean was used in the analyses. To determine the statistical significance of deforestation-induced changes, we applied the Student's *t*-test to each grid cell.

Regional differences of deforestation-induced changes are represented by root-mean-square error (RMSE), spatial correlation coefficient (SCC), and spatial standard deviation ratios (SSD). In addition, we used the composite evaluation index (Schuenemann and Cassano 2009; Tian et al., 2016) that combines the three indicators, RMSE, SCC, and SSD, as follow:

$$M_R = 1 - \frac{\sum_{i=1}^{n} r_i}{1 \times n \times m}, \quad (1)$$

where m is the number of subregions, n is the number of indicators, and r_i denotes the rank of each subregion for a certain indicator and ranges between 1 and m. If the r_i is equal to 1, representing deforestation has minimal impact on local tem-

Table 1. Basic information for the used CMIP6 models.

Model name	Institution/Country	Resolution (lon × lat)
ACCESS-ESM1-5	CSIRO/Australia	1. 875°×1.25°
BCC-CSM2-MR	BCC/China	T106 (1.125°×1.125°)
CMCC-ESM2	CMCC/Italy	1. 25°×0.938°
MPI-ESM1-2-LR	MPI-M/Germany	T63 (1. 875°×1.875°)
NorESM2-LM	NCC/Norway	2.5°×1.875°

Table 2. CMIP6 datasets.

Experiment ID	Experiment name	Experiment description	Years
Historical	Historical	Concentration driven (consistent with observations from 1850–2005)	1961–2014
SSP1-2.6	ScenarioMIP	Low radiative forcing scenario, Radiative forcing reaches a level of 2.6 W m^{-2} in 2100	2015–2100
SSP3-7.0	ScenarioMIP	Medium/high radiative forcing scenario, Radiative forcing reaches a level of 7.0 W m^{-2} in 2100	2015–2100
SSP126-SSP370Lu	LUMIP	Same as ScenarioMIP *ssp126* except use land use from *ssp370* (SSP3-7 deforestation scenario)	2015–99
SSP370-SSP126Lu	LUMIP	Same as ScenarioMIP *ssp370* except use land use from *ssp126* (SSP1-2.6 afforestation scenario)	2015–99

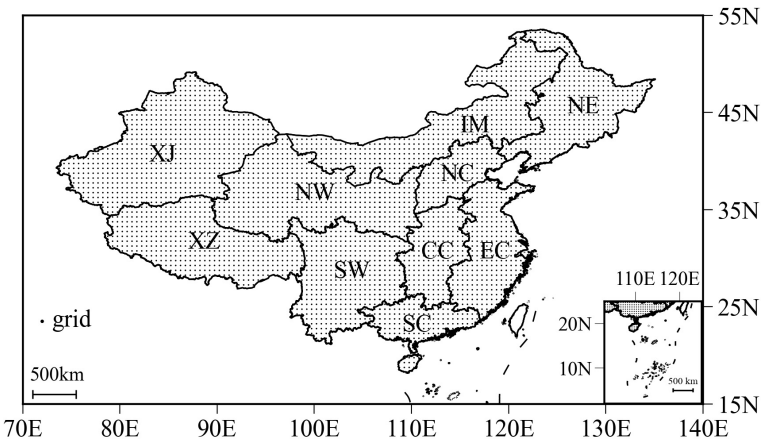

Fig. 1. The division of the ten subregions (NE: northeast China; NC: north China; IM: Inner Mongolia; EC: east China; CC: central China; SC: south China; SW: southwest China; NW: northwest China; XZ: Xizang; and XJ: Xinjiang).

perature change in a certain subregion, while a larger value of r_i corresponds to a larger response to deforestation. With this method, M_R can represent the overall impact of deforestation on local temperature change, with a smaller value in a certain subregion representing a greater impact of deforestation on temperature change.

3. Results

3.1. *Changes in surface air temperature (SAT)*

The deforestation-induced SAT change in China under different radiative forcing scenarios is of specific concern. Under the low radiative forcing scenario, the annual mean SAT changes due to deforestation show a continuing upward trend, with a magnitude of 1.0°C–3.5°C (Fig. 2). In contrast, the magnitude of deforestation-induced changes is comparatively small under the medium/high radiative forcing scenario, which indicates that the mean SAT response due to deforestation is more significant under the low radiative forcing scenario (Fig. 2a). At the monthly time scale, we find a net warming effect of deforestation by 1.5°C–3.0°C under the low radiative forcing scenario, and the warming is largest in January and smallest in March. However, the SAT is slightly cooling (–0.2°C–0°C) under the medium/high radiative forcing scenario, and the cooling is strongest in March and weakest in May. Our results indicate that the response of monthly SAT to the same deforestation can be opposite under different radiative forcing scenarios (Fig. 2b). At the seasonal time scale, the model ensemble mean shows significant warming (>2°C) induced by deforestation under the low radiative forcing scenario, while it shows a slight cooling (<–0.1°C) under the medium/high radiative forcing scenario (Fig. 2c). Overall, at the annual, monthly, and seasonal time scales, the SAT response to LULCC is much smaller under the medium/high radiative forcing scenario than the low radiative forcing scenario.

Analyses from CMIP6 ScenarioMIP simulations show that, compared with the historical period, greenhouse gases emissions warm most parts of China throughout a year. The SAT increase in northern China is larger than that in southern China, and a higher radiative forcing scenario would cause more warming (figure not shown). Further analysis regarding the deforestation effects shows more differences between the low and medium/high radiative forcing scenarios (Fig. 3). Under the low radiative forcing scenario, deforestation-induced SAT anomalies show statistically significant warming in all seasons, especially over the Tibetan Plateau. However, under the medium/high radiative forcing scenario, deforestation has a small impact on SAT in China and causes cooling in most regions. Thus, under the low radiative forcing scenario, the impact of deforestation would further amplify the effects of greenhouse gases in China, while the response of SAT is weak under the medium/high radiative forcing scenario.

Figure 4 presents the mean SAT changes of ten subregions in all seasons to further examine the regionally different effects of deforestation. Under the low radiative forcing scenario, the deforestation-induced SAT changes are positive in all subregions and have obvious regional differences. In particular, the positive SAT changes in southwest China (SW), northwest China (NW), and Xizang (XZ) are significantly greater than those in other subregions in all seasons, which indicates deforestation would lead to more significant warming in these subregions under the low radiative forcing scenario. In contrast, under the medium/high radiative forcing scenario, except for Xizang (XZ) in spring, other subregions have negative SAT changes in all seasons, that is, deforestation would cause cooling effects under the medium/high radiative forcing scenario, but the magnitude of cooling is slight (no more than –0.3°C).

Besides the mean SAT changes, we also analyze deforestation effects on interannual variability (Fig. 5) and trend (Fig. 6) of SAT under different warming scenarios. Under the low radiative forcing scenario, deforestation leads to an increase in the interannual variability of SAT, especially in

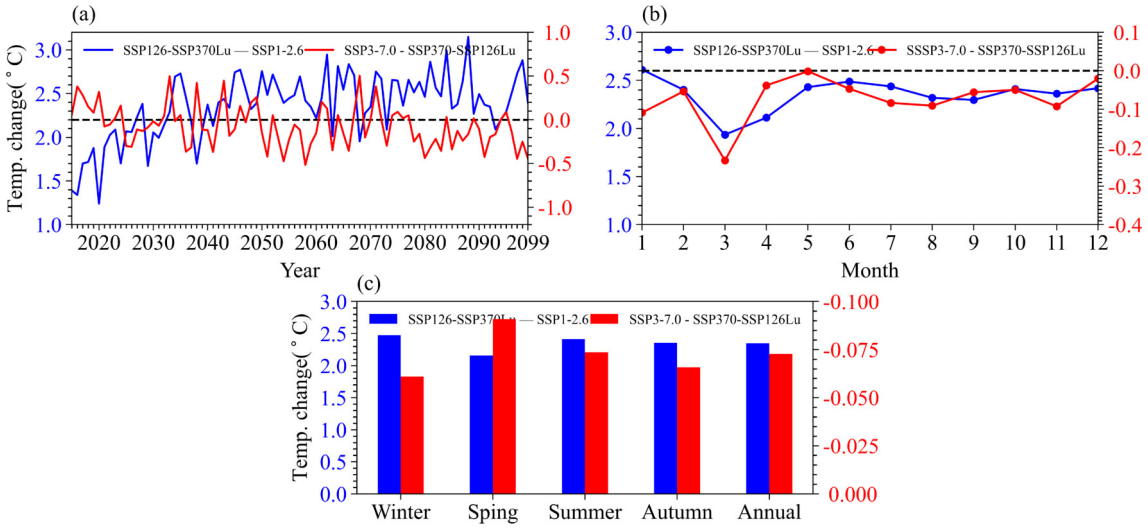

Fig. 2. Deforestation-induced regional averaged surface air temperature (SAT) changes (°C) over China under different emissions scenarios. (a) Time series from 2015 to 2099, (b) monthly mean during 2015–99, and (c) seasonal (DJF, MAM, JJA, and SON) mean during 2015–99. Blue: the low radiative forcing scenario, with values in the left *y*-axis; Red: the medium/high radiative forcing scenario, with values in the right *y*-axis.

southwest China and the eastern part of the Tibetan Plateau (Fig. 5a). The trend of SAT in China also shows a significant increase, especially in eastern China where it exceeds 0.1°C $(10\ yr)^{-1}$ (Fig. 6a). In contrast, under the medium/high radiative forcing scenario, the opposite response due to deforestation would decrease the interannual variability (Fig. 5b) and the trend of SAT (Fig. 6b) in most subregions. For each subregion, deforestation leads to an increase in interannual variability and a trend of SAT of similar magnitude as that under the low radiative forcing scenario. Under the medium/high radiative forcing scenario, the response is opposite, except for in the Xizang subregion. The interannual variability of mean SAT decreases in all subregions, and the magnitude is smaller than that under the low radiative forcing scenario (Fig. 5c). The analysis of SAT trend in subregions also leads to similar conclusions (Fig. 6c).

To quantitatively compare the response of SAT to deforestation in different subregions under different scenarios, we calculate the indices (RMSE, SCC, and SSD) of mean SAT and its interannual variability and trend. When RMSE is smaller (larger), SCC is larger (smaller), and SSD is closer to (far away from) 1, which means the SAT of a certain subregion is less (more) affected by deforestation. Under the low radiative forcing scenario, the RMSE of mean SAT has obvious regional differences, especially in Xizang, northwest and southwest China. The SCC of each subregion is more than 0.9, with similar magnitude among different subregions. The value of SSD ranges from 0.78 to 1.13, which means that the spatial consistency and similarity of mean SAT are high (Fig. 7a). The interannual variability and trend of SAT are also analyzed in a similar way. We find the RMSE of the interannual variability is similar in different regions, while the SCC and SSD are significantly different regionally. The SCC in Inner Mongolia, east China, south China, and Xinjiang exceeds 0.9, while the SCC in northwest China is about 0.4. The SSDs in Inner Mongolia, northwest China, and Xinjiang are close to 1, while the values in south and east China are far away from 1 (Fig. 7b).

The RMSE of the trend of SAT in each subregion is small, and the regional differences are not significant. However, the SCC and SSD both have obvious regional differences, with the largest positive value of SCC being in Xinjiang and south China and the largest negative value being in central China. SSD is close to 1 in Xizang, southwest and northwest China, while the value is far away from 1 in Inner Mongolia, east and south China (Fig. 7c). In terms of the composite evaluation index M_R, a smaller value represents a greater impact of deforestation on the regional SAT. Under the low radiative forcing scenario, we find the most significant SAT response to deforestation in northwest China and the smallest impact in Inner Mongolia (Fig. 7d).

Figure 8 shows the same analysis as in Fig. 7 but under the medium/high radiative forcing scenario. For the mean SAT, the RMSE of each subregion is small and the SCC and SSD are both close to 1, indicating no obvious regional differences. Therefore, deforestation has little impact on mean SAT changes in China under the medium/high radiative forcing scenario, which is quite different from the impact under the low radiative forcing scenario (Fig. 8a). The analyses of the interannual variability (Fig. 8b) and the trend of SAT (Fig. 8c) also obtain similar conclusions. Under the medium/high radiative forcing scenario, the RMSE is small and there are no obvious regional differences. The SCC and SSD in all subregions are close to 1 except in central China, indicating that deforestation has little impact on the interannual variability and trends of SAT. The values of M_R for each subregion are sequenced in ascending order: central China, south China, east China, north China, southwest

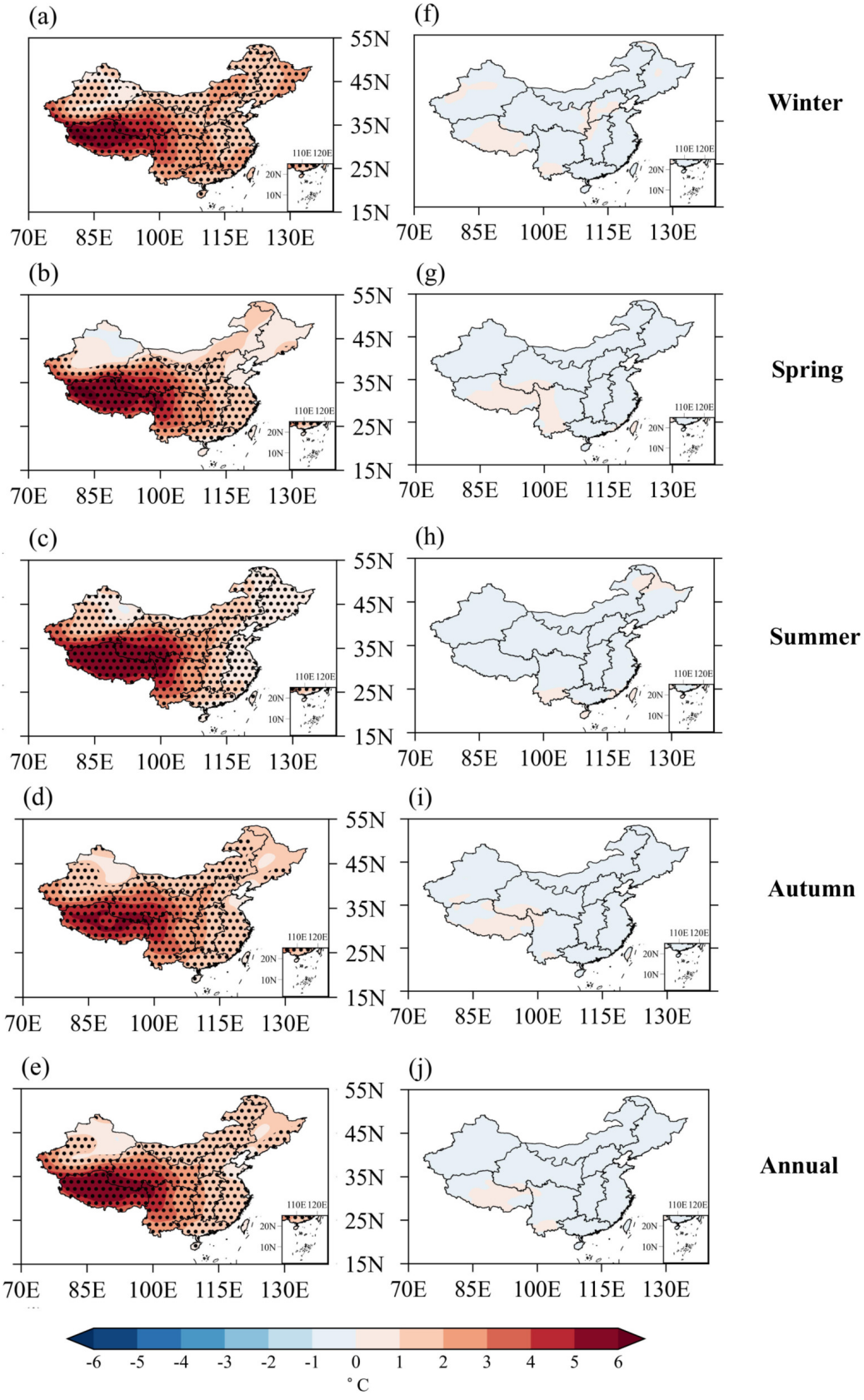

Fig. 3. Deforestation-induced annual and seasonal (DJF, MAM, JJA, and SON) mean SAT changes (°C) during 2015–99 over China under (a–e) the low radiative forcing scenario, and (f–j) the medium/high radiative forcing scenario. The black dots indicate changes are statistically significant at a 0.05 confidence level.

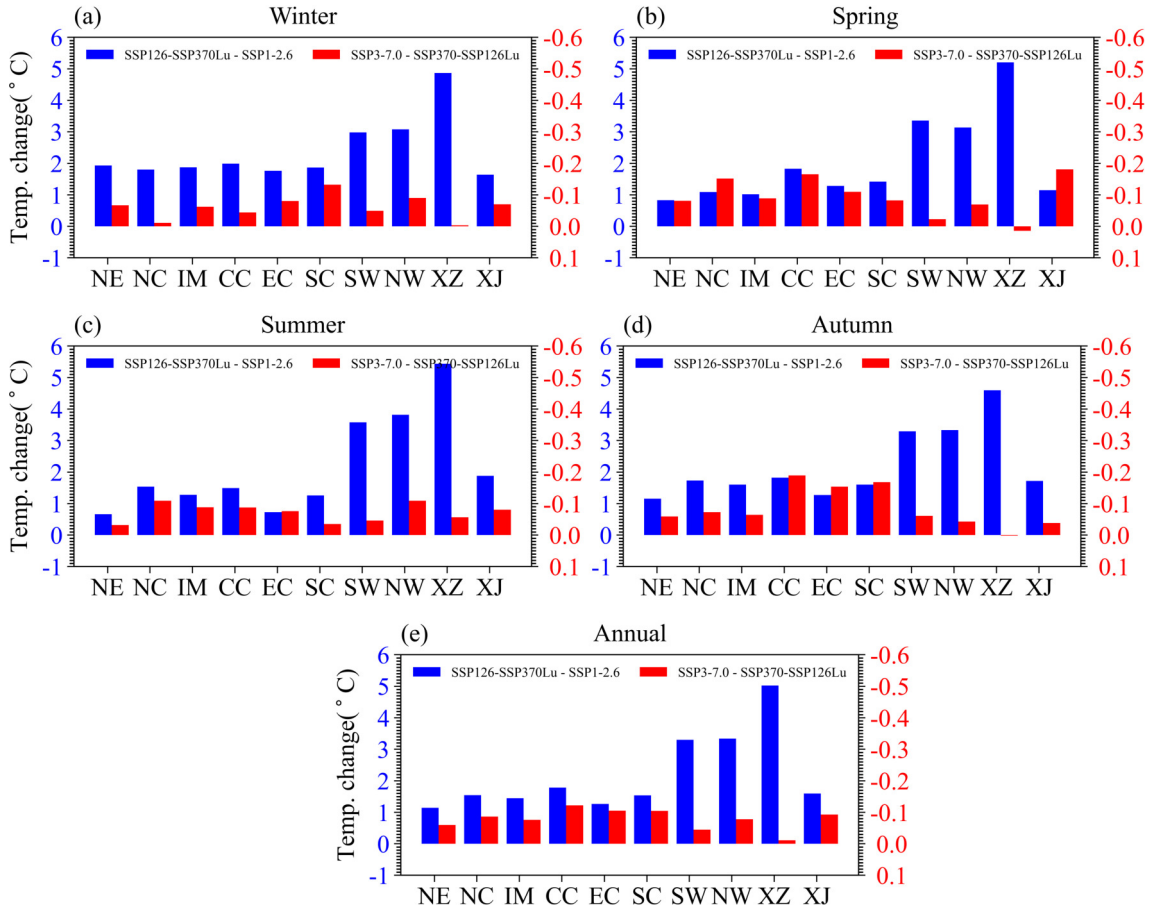

Fig. 4. Deforestation-induced subregional annual and seasonal (DJF, MAM, JJA, and SON) mean SAT changes (°C) during 2015–99 under different emissions scenarios (blue bar: the low radiative forcing scenario, with values in the left *y*-axis; red bar: the medium/high radiative forcing scenario, with values in the right *y*-axis).

China, Xinjiang, Inner Mongolia, northeast China, northwest China, and Xizang. Thus, under the medium/high radiative forcing scenario, deforestation has the largest impact on SAT in central China and the smallest impact in the Xizang subregion (Fig. 8d).

3.2. *Changes in precipitation*

We also examine the impacts of deforestation on precipitation under different radiative forcing scenarios (Fig. 9). Under the low radiative forcing scenario, deforestation leads to a significant decrease in annual precipitation, while the precipitation has no obvious trend under the medium/high radiative forcing scenario (Fig. 9a). Our results indicate that the impact of deforestation on annual precipitation is uncertain under the medium/high radiative forcing scenario. At the monthly scale, the precipitation changes under different scenarios are basically opposite (Fig. 9b). Under the low radiative forcing scenario, deforestation leads to decreased precipitation in most months except for January, November, and December. The largest reduction is found in July, reaching approximately –0.5 mm d^{-1}. However, under the medium/high radiative forcing scenario, we find a slight increase in deforestation-induced precipitation. At the seasonal scale, deforestation-induced precipitation changes are opposite under different forcing scenarios except for in winter. The most significant changes are found in summer in both scenarios, and the impact of deforestation on precipitation is more significant than under the low radiative forcing scenario (Fig. 9c).

We further analyze the impact of deforestation on the regional differences of seasonal precipitation in China under different warming scenarios. Under the low radiative forcing scenario, deforestation would lead to a significant decrease (increase) in precipitation in southern (northern) China in winter (Fig. 10a), spring (Fig. 10b), and autumn (Fig. 10d). In summer (Fig. 10c), the precipitation decreases in most parts of China except for Xinjiang, especially in southwest China and Xizang (>1.5 mm d^{-1}). However, under the medium/high radiative forcing scenario, the regional impact of deforestation on seasonal precipitation in China is uncertain, and the precipitation changes in most regions are not significant (Figs. 10f–j).

The spatial patterns of precipitation anomaly are divided into three periods: near term (2021–40), middle term (2041–70), and long term (2071–99). In the three periods, the difference of forest area between the low and medium/high radiative forcing scenarios is about 2×10^6 km^2, 5×10^6 km^2, and 8×10^6 km^2, respectively. Figure 11 shows

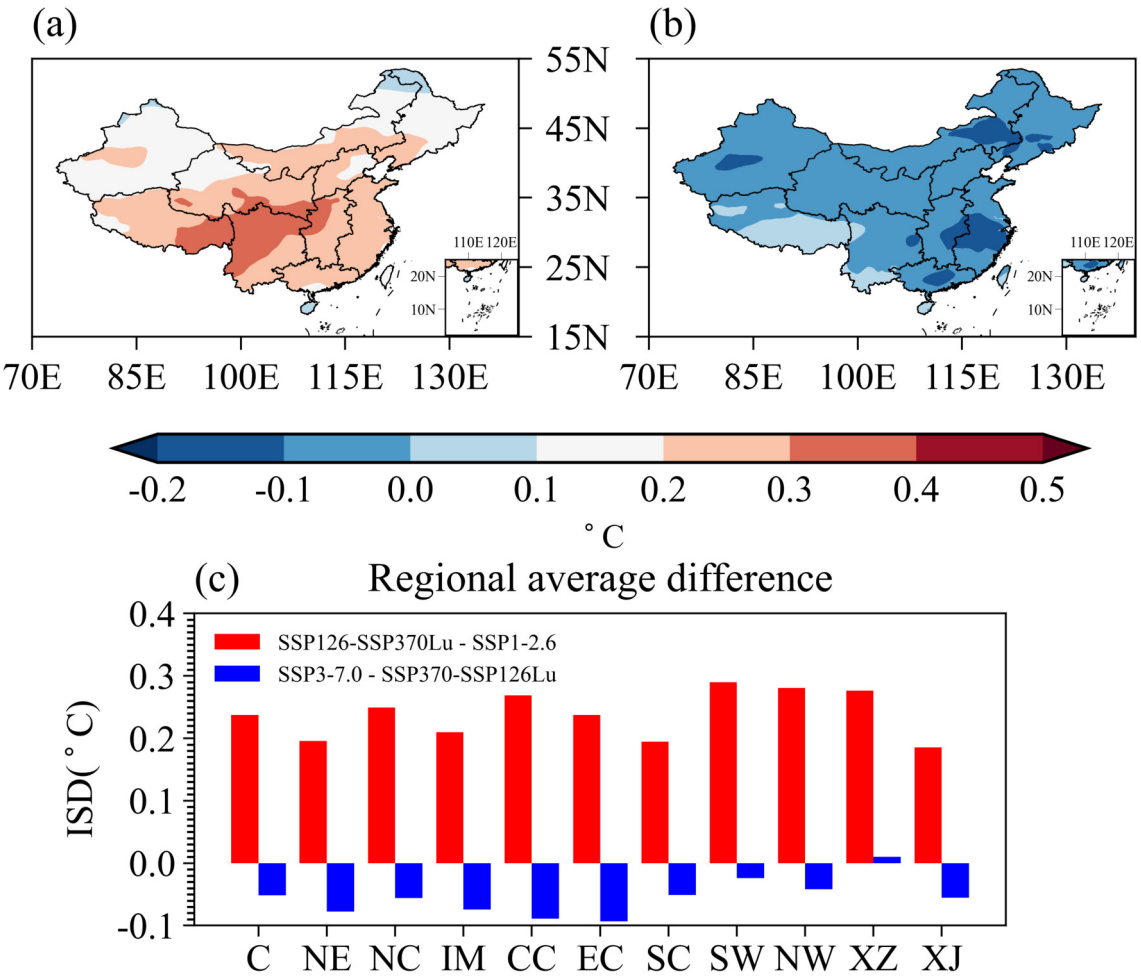

Fig. 5. Deforestation-induced interannual variability of SAT change (°C) during 2015–99 under (a) the low radiative forcing scenario, (b) the medium/high radiative forcing scenario, and (c) average over China (C) and the ten subregions.

the spatial patterns of deforestation-induced precipitation anomaly in China under different warming backgrounds. Under the low radiative forcing scenario, the spatial pattern of deforestation-induced precipitation anomaly is similar in the three periods, with a significant decrease in southern China and an increase in northern China, especially in Xinjiang. As we know, under the ScenarioMIP SSP1-2.6 scenario, global warming would lead to decreased precipitation in winter in southern China and increased precipitation in other seasons over most parts of China. In the near term, precipitation decreases in southern China and increases in northern China, while in the middle term and the long term, precipitation increases in most subregions (figure not shown). Compared with the ScenarioMIP SSP1-2.6 scenario, deforestation would amplify the spatial difference on precipitation anomaly between southern and northern China under the low radiative forcing scenario. However, under the medium/high radiative forcing scenario, the impacts of deforestation on precipitation changes in China are not significant, and the spatial differences are small.

Comparing the mean precipitation of 10 subregions in different periods, we find that, under the low radiative forcing scenario, deforestation-induced precipitation anomaly of all subregions has a relatively consistent pattern in the near term, middle term, and long term (Figs. 12a–c). Except for the weak increase in northeast China, Inner Mongolia, and Xinjiang, deforestation reduces precipitation in other subregions. Regionally, the significant precipitation change is found in Xizang, southwest, central, east, and south China. However, under the medium/high radiative forcing scenario, deforestation-induced precipitation anomaly is less than 0.1 mm d^{-1} in different periods over most subregions, and there are obvious regional differences. In the near term, the mean precipitation would increase in south China, north China, Inner Mongolia, and northwest China, while it would decrease in northeast China, east China, and Xizang (Fig. 12a). In the middle term, precipitation decreases in south China with a magnitude of –0.1 mm d^{-1} and increases in southwest China with a magnitude of 0.08 mm d^{-1} (Fig. 12b). In the long term, except for the slight decrease in northeast China and Xizang, mean precipitation will increase in most subregions, especially in south and east China with a magnitude of 0.15 mm d^{-1} (Fig. 12c).

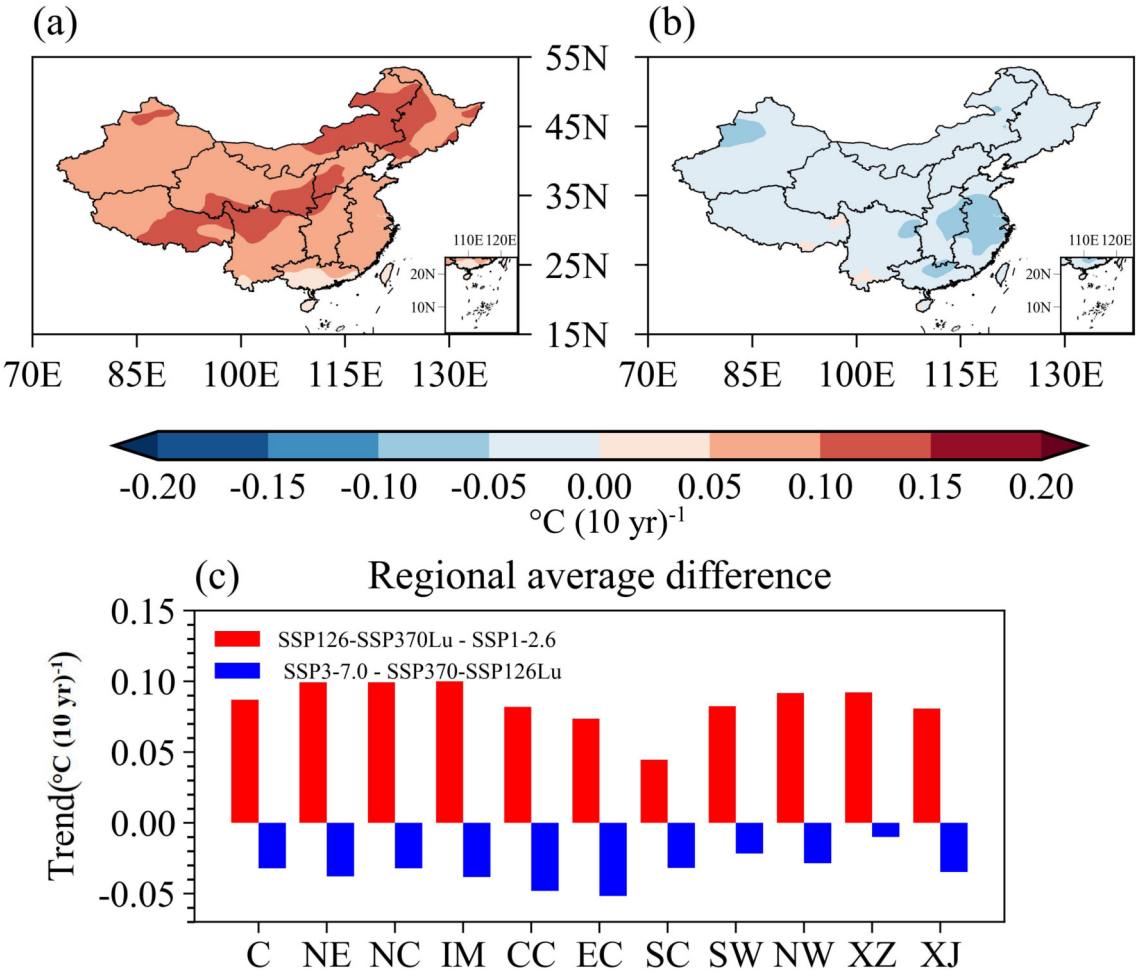

Fig. 6. As in Fig. 5, but for the trend of surface air temperature change [°C (10 yr)$^{-1}$].

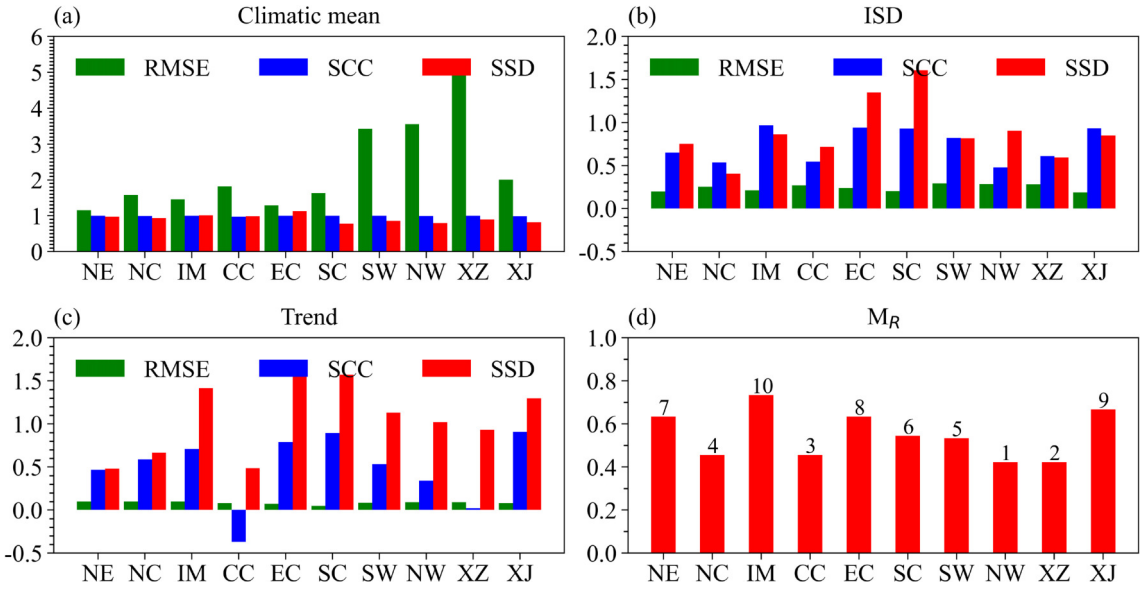

Fig. 7. Regional averaged changes of deforestation-induced SAT parameters during 2015–2099 under the low radiative forcing scenario. (a) mean SAT (°C), (b) interannual variability (°C), and (c) trend [°C (10 yr)$^{-1}$]; and (d) M_R value of ten subregions. Green, blue, and red bars in (a–c) denote RMSE, SCC, and SSD, respectively. The numbers above the bars in (d) denote the response to deforestation with descending sequence over ten subregions under the low radiative forcing scenario.

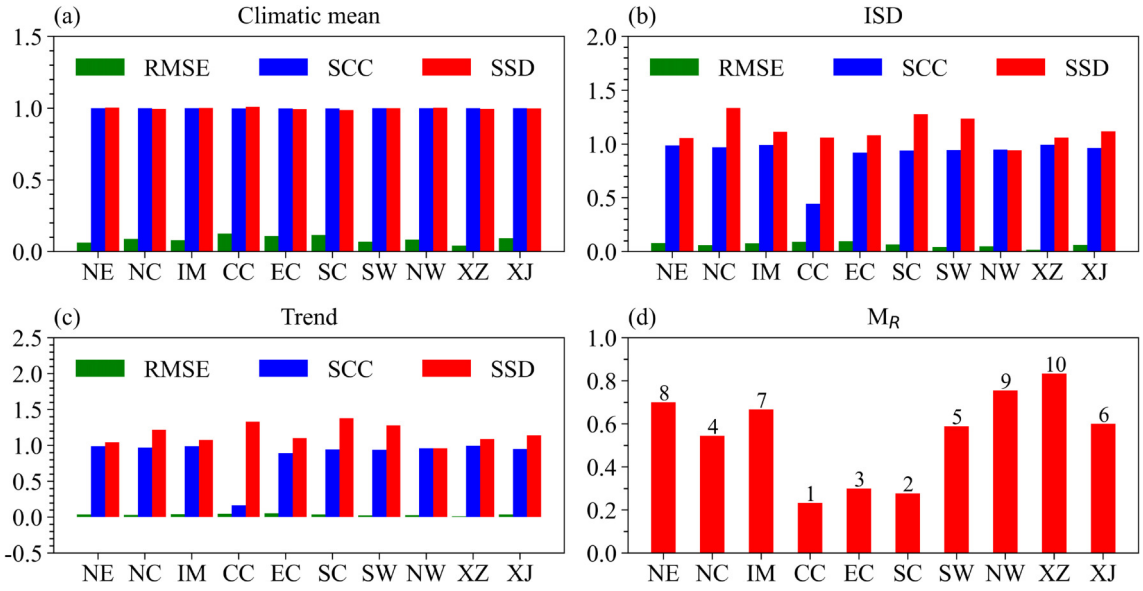

Fig. 8. As in Fig. 7, but under the medium/high radiative forcing scenario.

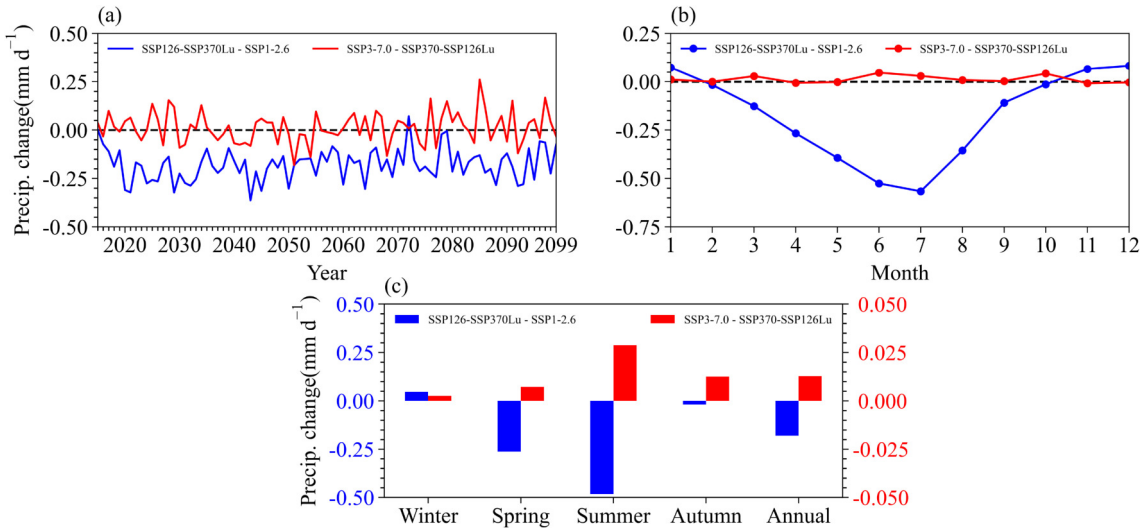

Fig. 9. Deforestation-induced regional averaged precipitation change (mm d^{-1}) over China under different emissions scenarios. (a) Time series from 2015 to 2099, (b) monthly mean during 2015–99, and (c) seasonal (DJF, MAM, JJA, and SON) mean during 2015–99. Blue: the low radiative forcing scenario, with values in the left *y*-axis; Red: the medium/high radiative forcing scenario, with values in the right *y*-axis.

3.3. *Mechanisms analysis*

Our results show that the impacts of deforestation on temperature and precipitation have different responses under different background climates. From the viewpoint of land surface energy budget and partitioning, we analyzed the changes of net radiation and latent/sensible heat fluxes associated with the variations of surface air temperature and precipitation under the different global warming scenarios.

As seen from Figs. 13a–d, deforestation leads to a reduction in precipitation and latent heat fluxes in southern China under the low radiative forcing scenario. It is known that deforestation would lead to an increased albedo and hence a reduction in net radiation. In contrast, the drought caused by deforestation would lead to an increase in sensible heat fluxes and thus a warming of the atmosphere. Therefore, deforestation has a greater warming effect in regions with larger decreased precipitation, where the impacts of deforestation are dominantly controlled by hydrological processes rather than by albedo changes. In northern China, deforestation would increase the precipitation under the low radiative forcing scenario and induce more latent heat release and a cooling effect. In addition, warmer climates decrease snow and surface albedo, which increase the net radiation and raise the temperature, thus partially negating the cooling due to precipitation.

In contrast, as shown in Figs. 13e–h, deforestation would increase the albedo and decrease the net radiation in southern China under a warmer scenario. Additionally, the

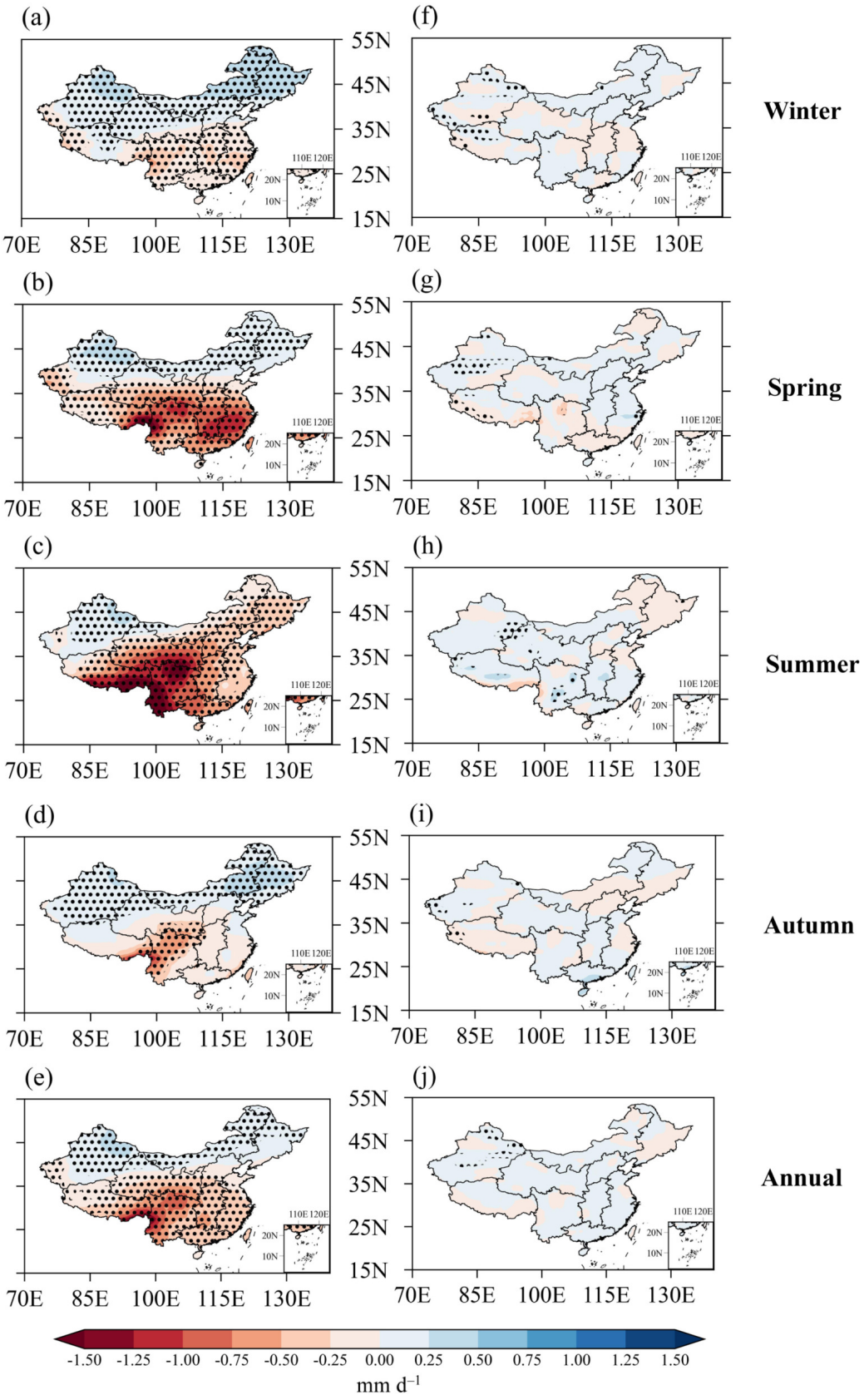

Fig. 10. Deforestation-induced annual and seasonal (DJF, MAM, JJA, and SON) mean precipitation changes (mm d^{-1}) during 2015–99 over China under (a–e) the low radiative forcing scenario, and (f–j) the medium/high radiative forcing scenario. The black dots indicate changes are statistically significant at a 0.05 confidence level.

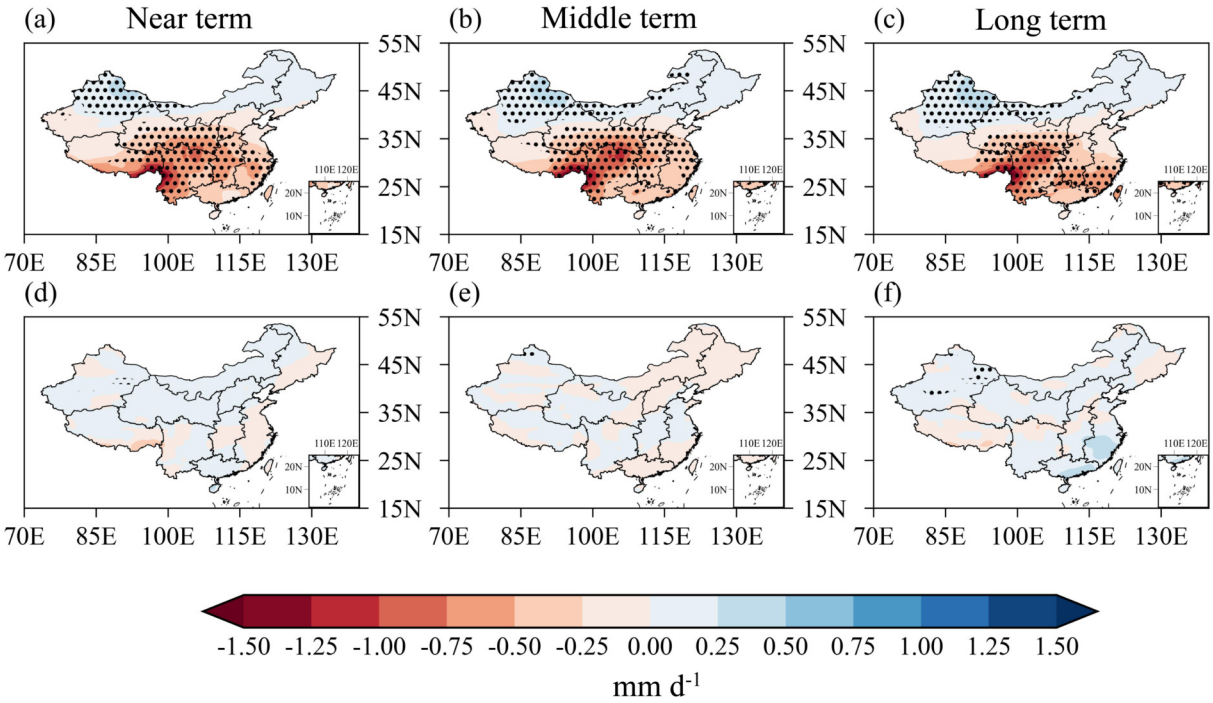

Fig. 11. Deforestation-induced annual mean precipitation changes (mm d^{-1}) in the near term, middle term, and long term under (a–c) the low radiative forcing scenario and (d–f) the medium/high radiative forcing scenario. The black dots indicate changes are statistically significant at a 0.05 confidence level.

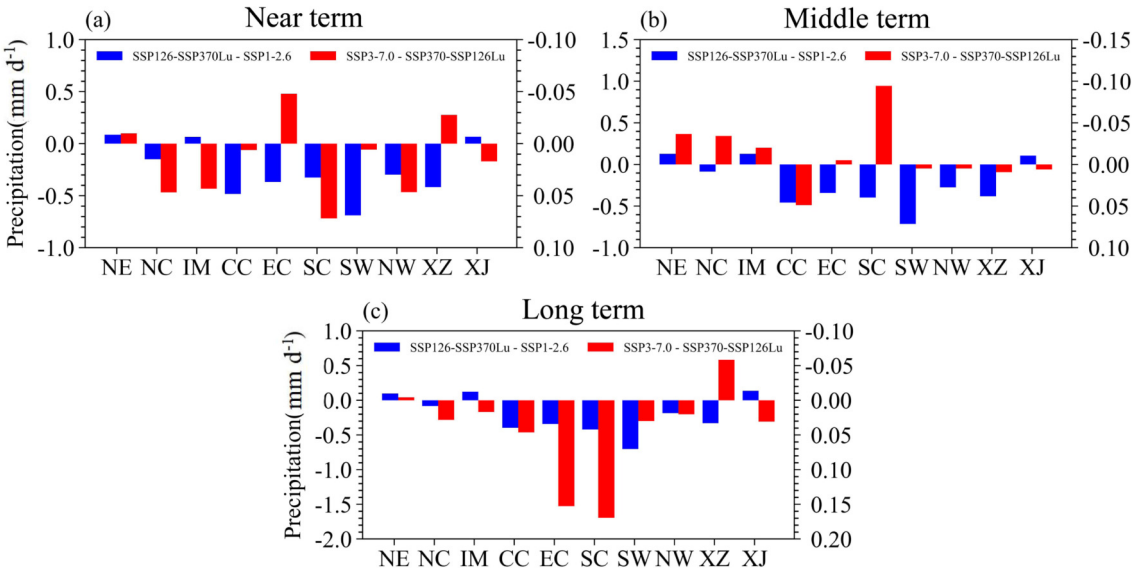

Fig. 12. Deforestation-induced annual mean precipitation changes (mm d^{-1}) in the (a) near term, (b) middle term, and (c) long term over 10 subregions under different emissions scenarios (blue bar: the low radiative forcing scenario, with values in the left *y*-axis; red bar: the medium/high radiative forcing scenario, with values in the right *y*-axis).

increased precipitation would lead to latent heat flux increases in northwest China and Inner Mongolia and then affect the partition of net radiation between latent heat and sensible heat fluxes, which would eventually lead to a cooling effect in most parts of China. There is an opposite response to the temperature changes under the low radiative forcing scenario.

Pitman et al. (2011) proposed that the background climate plays an important role in determining the impacts of LULCC on regional climate. Hua and Chen (2013) and Li et al. (2016) also investigated the mechanisms of regional impacts of LULCC on climate changes with consideration of different atmospheric CO_2 concentrations. Their results indicate that the level of CO_2 influences changes in surface albedo and hydrometeorology, which determine the impacts of LULCC in the form of deforestation. Our results are basi-

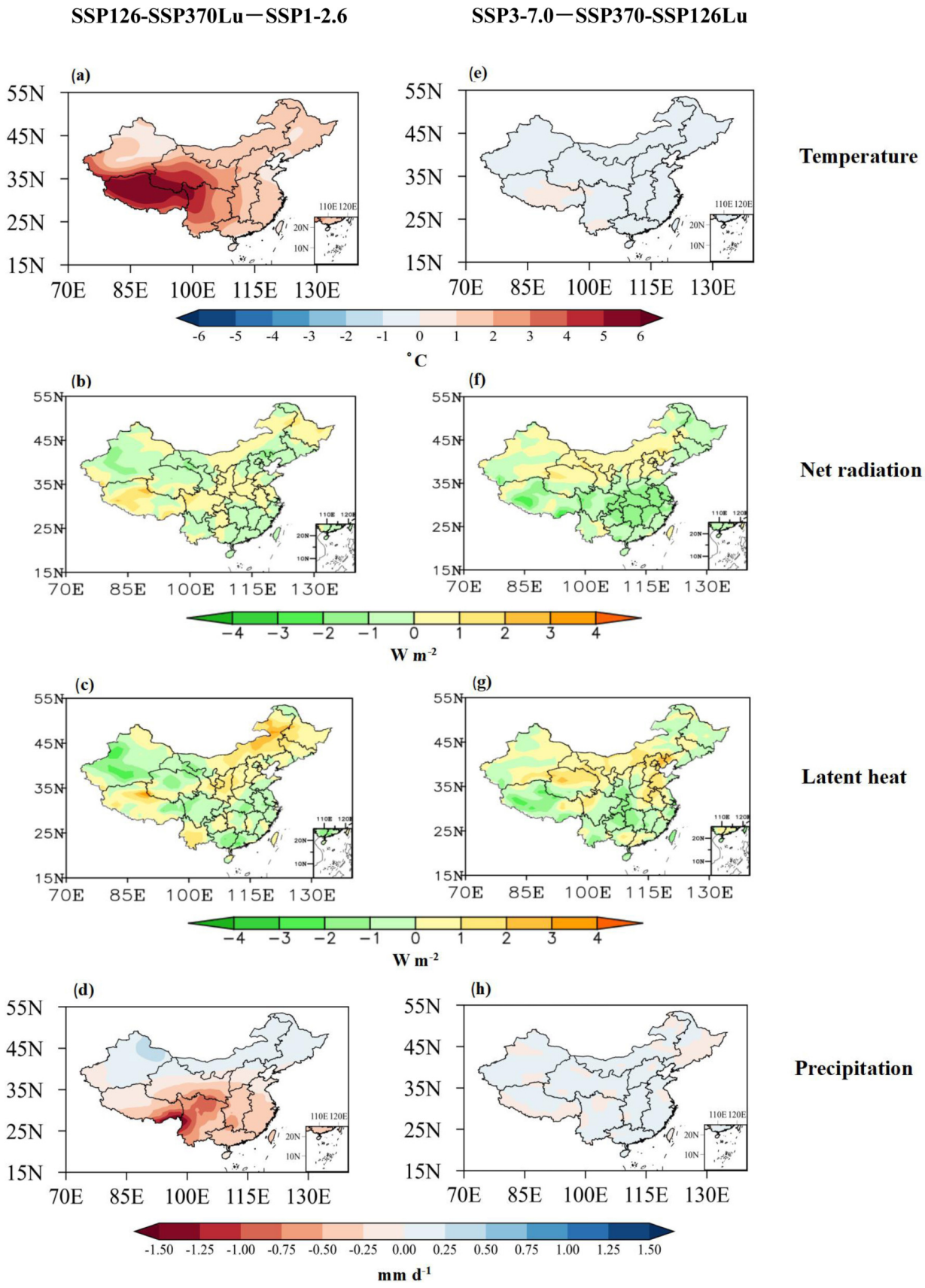

Fig. 13. Deforestation-induced changes of annual mean (a, e) SAT (°C), (b, f) net radiation (W m^{-2}), (c, g) latent heat (W m^{-2}), and (d, h) precipitation (mm d^{-1}) during 2015–99 over China under (a–d) the low radiative forcing scenario and (e–h) the medium/high radiative forcing scenario.

cally in line with the conclusions of previous studies, which highlights the importance of interactions among the land surface energy balance, terrestrial ecosystem, and hydrologic cycle for better understanding the overall impacts of LULCC under changing climate background.

4. Conclusions and discussion

Based on the multimodel climate experiments from the Land Use Model Intercomparison Project (LUMIP), this study investigates the climate responses of temperature and precipitation in China to global forest area change under different climate warming backgrounds.

The temperature changes due to deforestation have opposite responses under different climate warming backgrounds. Under the low radiative forcing scenario, deforestation would lead to an increase in the annual mean SAT and its interannual variability and trend in all seasons. In contrast, deforestation would lead to cooling in most parts of China, and decrease the interannual variability and trend of SAT under the medium/high radiative forcing scenario, but the magnitude of temperature change is less than that under the low radiative forcing scenario. Moreover, deforestation-induced SAT change shows significant regional differences. Under the low radiative forcing scenario, deforestation has a significant impact on SAT change in northwest China, Xizang, and central China, while the significant subregions are central, south, and east China under the medium/high radiative forcing scenario.

For precipitation, the responses to deforestation are also different under the two emissions scenarios. Under the low radiative forcing scenario, deforestation would lead to a significant increase in precipitation in northern China but a significant decrease in southern China, especially during spring and summer. This precipitation pattern can be found in the near term (2021–40), middle term (2041–70) and long term (2071–99). However, under the medium/high radiative forcing scenario, changes in precipitation are weaker, and there are no significant regional differences. Precipitation increases are found over most parts of China both in the near term and long term, while precipitation decreases are found in the middle term, especially in south, north, and northeast China.

In general, the impact of forest cover change on temperature and precipitation under the low radiative forcing scenario is significantly greater than that under the medium/high radiative forcing scenario. It is consistently shown that the background climate plays an important role in the regional impact of forest cover change. Our results show that under the low radiative forcing scenario, deforestation leads to increased temperature and decreased precipitation in most parts of China, and the effects are equivalent to the greenhouse effect. Therefore, under the low radiative forcing scenario, afforestation would mitigate the effects of greenhouse gases to a certain extent. However, under the higher emissions scenario, the response of temperature and precipitation change over China is uncertain, and the magnitude is negligible compared with the greenhouse gases effect, indicating that afforestation could not effectively improve the greenhouse gases effect in this scenario. This study reveals the importance of different climate backgrounds in controlling LULCC effects on the regional climate, and both changes need to be considered in future climate projection. It should be noted that the analysis conducted in this study includes some preliminary findings, and there are still some limitations and uncertainties worthy of further investigation. The capacity of climate models to correctly capture the changes in rainfall and temperature relative to LULCC probably affects many aspects of our results, which presents a challenge for the development and improvement of climate models. In addition, how the time evolution of LULCC affects local changes in rainfall and temperature at regional scales is a problem deserving further study.

Acknowledgements. This study is jointly supported by the National Natural Science Foundation of China under Grant No. 41975081, the Research Funds for the Frontiers Science Center for Critical Earth Material Cycling Nanjing University, and the Fundamental Research Funds for the Central Universities (Grant No. 020914380103).

Data Availability Statement. The CMIP6 model data used in this study can be accessed at the ESGF portal (https://esgf-node.llnl.gov/projects/esgf-llnl/).

REFERENCES

Alkama, R., and A. Cescatti, 2016: Biophysical climate impacts of recent changes in global forest cover. *Science*, **351**, 600–604, https://doi.org/10.1126/science.aac8083.

Arora, V. K., and A. Montenegro, 2011: Small temperature benefits provided by realistic afforestation efforts. *Nature Geoscience*, **4**(8), 514–518, https://doi.org/10.1038/ngeo1182.

Bonan, G. B., 2008: Forests and climate change: Forcings, feedbacks, and the climate benefits of forests. *Science*, **320**(5882), 1444–1449, https://doi.org/10.1126/science.1155121.

Boysen, L. R., and Coauthors, 2020: Global climate response to idealized deforestation in CMIP6 models. *Biogeosciences*, **17**(22), 5615–5638, https://doi.org/10.5194/bg-17-5615-2020.

Brovkin, V., and Coauthors, 2013: Effect of anthropogenic land-use and land-cover changes on climate and land carbon storage in CMIP5 projections for the twenty-first century. *J. Climate*, **26**(18), 6859–6881, https://doi.org/10.1175/jcli-d-12-00623.1.

Bryan, B. A., and Coauthors, 2018: China's response to a national land-system sustainability emergency. *Nature*, **559**, 193–204, https://doi.org/10.1038/s41586-018-0280-2.

Chen, H. S., X. Li, and W. J. Hua, 2015: Numerical simulation of the impact of land use/land cover change over China on regional climates during the last 20 years. *Chinese Journal of Atmospheric Sciences*, **39**(2), 357–369, https://doi.org/10.3878/j.issn.1006-9895.1404.14114. (in Chinese with English abstract)

Davin, E. L., and N. de Noblet-Ducoudré, 2010: Climatic impact of global-scale deforestation: Radiative versus nonradiative processes. *J. Climate*, **23**, 97–112, https://doi.org/10.1175/2009JCLI3102.1.

Devaraju, N., N. de Noblet-Ducoudré, B. Quesada, and G. Bala, 2018: Quantifying the relative importance of direct and indirect biophysical effects of deforestation on surface temperature and teleconnections. *J. Climate*, **31**, 3811–3829, https://doi.org/10.1175/JCLI-D-17-0563.1.

Dixon, R. K., A. M. Solomon, S. Brown, R. A. Houghton, M. C. Trexier, and J. Wisniewski, 1994: Carbon pools and flux of global forest ecosystems. *Science*, **263**, 185–190, https://doi.org/10.1126/science.263.5144.185.

Duveiller, G., J. Hooker, and A. Cescatti, 2018: The mark of vegetation change on Earth's surface energy balance. *Nat. Commun.*, **9**, 679, https://doi.org/10.1038/s41467-017-02810-8.

FAO, 2009: *State of the World's Forests 2009*. Rome, 168 pp.

Foley, J. A., and Coauthors, 2005: Global consequences of land use. *Science*, **309**(5734), 570–574, https://doi.org/10.1126/science.1111772.

Fu, B. J., S. Wang, Y. Liu, J. B. Liu, W. Liang, and C. Y. Miao, 2017: Hydrogeomorphic ecosystem responses to natural and anthropogenic changes in the Loess Plateau of China. *Annual Review of Earth and Planetary Sciences*, **45**, 223–243, https://doi.org/10.1146/annurev-earth-063016-020552.

Ge, J., W. D. Guo, A. J. Pitman, M. G. De Kauwe, X. L. Chen, and C. B. Fu, 2019: The nonradiative effect dominates local surface temperature change caused by afforestation in China. *J. Climate*, **32**, 4445–4471, https://doi.org/10.1175/JCLI-D-18-0772.1.

Held, I. M., and B. J. Soden, 2006: Robust responses of the hydrological cycle to global warming. *J. Climate*, **19**, 5686–5699, https://doi.org/10.1175/JCLI3990.1.

Hong, T., J. J. Wu, X. B. Kang, M. Yuan, and L. Duan, 2022: Impacts of different land use scenarios on future global and regional climate extremes. *Atmosphere*, **13**, 995, https://doi.org/10.3390/atmos13060995.

Hu, Z. H., Z. F. Xu, and Z. G. Ma, 2018: The impact of land use/land cover changes under different greenhouse gas concentrations on climate in Europe. *Climatic and Environmental Research*, **23**(2), 176–184, https://doi.org/10.3878/j.issn.1006-9585.2017.17010. (in Chinese with English abstract)

Hua, W. J., and H. S. Chen, 2013: Recognition of climatic effects of land use/land cover change under global warming. *Chinese Science Bulletin*, **58**(31), 3852–3858, https://doi.org/10.1007/s11434-013-5902-3.

Hua, W. J., H. S. Chen, and X. Li, 2015: Effects of future land use change on the regional climate in China. *Science China Earth Sciences*, **58**(10), 1840–1848, https://doi.org/10.1007/s11430-015-5082-x.

Hua, W. J., S. Y. Liu, and H. S. Chen, 2021: Short commentary on Land Use Model Intercomparison Project (LUMIP). *Transactions of Atmospheric Sciences*, **44**(6), 818–824, https://doi.org/10.13878/j.cnki.dqkxxb.20210413001. (in Chinese with English abstract)

Hua, W. J., and Coauthors, 2017: Observational quantification of climatic and human influences on vegetation greening in China. *Remote Sensing*, **9**(5), 425, https://doi.org/10.3390/rs9050425.

Huang, H. L., Y. K. Xue, N. Chilukoti, Y. Liu, G. Chen, and I. Diallo, 2020: Assessing global and regional effects of reconstructed land-use and land-cover change on climate since 1950 using a coupled land-atmosphere-ocean model. *J. Climate*, **33**(20), 8997–9013, https://doi.org/10.1175/jcli-d-20-0108.1.

Hurtt, G. C., S. Frolking, M. G. Fearon, B. Moore, E. Shevliakova, S. Malyshev, S. W. Pacala, and R. A. Houghton, 2006: The underpinnings of land-use history: Three centuries of global gridded land-use transitions, wood-harvest activity, and resulting secondary lands. *Global Change Biology*, **12**(7), 1208–1229, https://doi.org/10.1111/j.1365-2486.2006.01150.x.

IPCC, 2021: *Climate change 2021: The physical science basis. Contribution of Working Group I to the Sixth Assessment Report of the Intergovernmental Panel on Climate Change.* V. Masson-Delmotte, et al., Eds., Cambridge University Press, Cambridge, United Kingdom and New York, NY, USA, 2391pp. https://doi.org/10.1017/9781009157896.

Lawrence, D. M., and Coauthors, 2016: The land use model intercomparison project (LUMIP) contribution to CMIP6: Rationale and experimental design. *Geoscientific Model Development*, **9**(9), 2973–2998, https://doi.org/10.5194/gmd-9-2973-2016.

Lawrence, P. J., and Coauthors, 2012: Simulating the biogeochemical and biogeophysical impacts of transient land cover change and wood harvest in the Community Climate System Model (CCSM4) from 1850 to 2100. *J. Climate*, **25**(9), 3071–3095, https://doi.org/10.1175/jcli-d-11-00256.1.

Lee, X., and Coauthors, 2011: Observed increase in local cooling effect of deforestation at higher latitudes. *Nature*, **479**(7373), 384–387, https://doi.org/10.1038/nature10588.

Li, Y., M. S. Zhao, S. Motesharrei, Q. Z. Mu, E. Kalnay, and S. C. Li, 2015: Local cooling and warming effects of forests based on satellite observations. *Nature Communications*, **6**, 6603, https://doi.org/10.1038/ncomms7603.

Li, Y., N. De Noblet-Ducoudré, E. L. Davin, S. Motesharrei, N. Zeng, S. C. Li, and E. Kalnay, 2016: The role of spatial scale and background climate in the latitudinal temperature response to deforestation. *Earth System Dynamics*, **7**(1), 167–181, https://doi.org/10.5194/esd-7-167-2016.

Liu, J. G., S. X. Li, Z. Y. Ouyang, C. Tam, and X. D. Chen, 2008: Ecological and socioeconomic effects of China's policies for ecosystem services. *Proceedings of the National Academy of Sciences of the United States of America*, **105**, 9477–9482, https://doi.org/10.1073/pnas.0706436105.

Lorenz, R., A. J. Pitman, and S. A. Sisson, 2016: Does Amazonian deforestation cause global effects; can we be sure? *J. Geophys. Res: Atmos.*, **121**(10), 5567–5584, https://doi.org/10.1002/2015jd024357.

Luo, X., J. Ge, W. D. Guo, L. Fan, C. R. Chen, Y. Liu, and L. M. Yang, 2022: The biophysical impacts of deforestation on precipitation: Results from the CMIP6 model intercomparison. *J. Climate*, **35**, 3293–3311, https://doi.org/10.1175/JCLI-D-21-0689.1.

Mao, H. Q., X. D. Yan, and Z. Xiong, 2011: An overview of impacts of land use change on climate. *Climatic and Environmental Research*, **16**(4), 513–524, https://doi.org/10.3878/j.issn.1006-9585.2011.04.12. (in Chinese with English abstract)

Perugini, L., L. Caporaso, S. Marconi, A. Cescatti, B. Quesada, N. de Noblet-Ducoudré, J. I. House, and A. Arneth, 2017: Biophysical effects on temperature and precipitation due to land cover change. *Environmental Research Letters*, **12**, 053002,

https://doi.org/10.1088/1748-9326/aa6b3f.

Pielke, R. A., and R. Avissar, 1990: Influence of landscape structure on local and regional climate. *Landscape Ecology*, **4**(2), 133−155, https://doi.org/10.1007/BF00132857.

Pielke, R. A., and Coauthors, 2011: Land use/land cover changes and climate: Modeling analysis and observational evidence. *WIREs Climate Change*, **2**(6), 828−850, https://doi.org/10.1002/wcc.144.

Pitman, A. J., F. B. Avila, G. Abramowitz, Y. P. Wang, S. J. Phipps, and N. de Noblet-Ducoudré, 2011: Importance of background climate in determining impact of land-cover change on regional climate. *Nature Climate Change*, **1**, 472−475, https://doi.org/10.1038/nclimate1294.

Pitman, A. J., and Coauthors, 2009: Uncertainties in climate responses to past land cover change: First results from the LUCID intercomparison study. *Geophys. Res. Lett.*, **36**, L14814, https://doi.org/10.1029/2009GL039076.

Pitman, A. J., and Coauthors, 2012: Effects of land cover change on temperature and rainfall extremes in multi-model ensemble simulations. *Earth System Dynamics*, **3**, 213−231, https://doi.org/10.5194/esd-3-213-2012.

Schuenemann, K. C., and J. J. Cassano, 2009: Changes in synoptic weather patterns and Greenland precipitation in the 20th and 21st centuries: 1. Evaluation of late 20th century simulations from IPCC models. *J. Geophys. Res.: Atmos.*, **114**, D20113, https://doi.org/10.1029/2009JD011705.

Shao, P., and X. D. Zeng, 2012: Progress in the study of the effects of land use and land cover change on the climate system. *Climatic and Environmental Research*, **17**(1), 103−111, https://doi.org/10.3878/j.issn.1006-9585.2011.10029. (in Chinese with English abstract)

Sun, G. D., and M. Mu, 2013: Using the Lund-Potsdam-Jena model to understand the different responses of three woody plants to land use in China. *Adv. Atmos. Sci.*, **30**(2), 515−524, https://doi.org/10.1007/s00376-012-2011-1.

Taylor, C. M., E. F. Lambin, N. Stephenne, R. J. Harding, and R. L. H. Essery, 2002: The influence of land use change on climate in the Sahel. *J. Climate*, **15**(24), 3615−3629, https://doi.org/10.1175/1520-0442(2002)015<3615:TIOLUC>2.0.CO;2.

Tian, L., Z. H. Jiang, and W. L. Chen, 2016: Evaluation of summer average circulation simulation over East Asia by CMIP5 climate models. *Climatic and Environmental Research*, **21**(4), 380−392, https://doi.org/10.3878/j.issn.1006-9585.2016.13089. (in Chinese with English abstract)

Wan, H. C., and Z. Zhong, 2014: Ensemble simulations to investigate the impact of large-scale urbanization on precipitation in the lower reaches of Yangtze River Valley, China. *Quart. J. Royal. Meteor. Soc.*, **140**, 258−266, https://doi.org/10.1002/qj.2125.

Wang, A. H., Y. Miao, and X. L. Shi, 2021: Short commentary on the Land-Use Model Intercomparison Project (LUMIP). *Climate Change Research*, **17**(3), 367−373, https://doi.org/10.12006/j.issn.1673-1719.2020.170. (in Chinese with English abstract)

Xu, Z. F., and Z. L. Yang, 2017: Relative impacts of increased greenhouse gas concentrations and land cover change on the surface climate in arid and semi-arid regions of China. *Climatic Change*, **144**, 491−503, https://doi.org/10.1007/s10584-017-2025-x.

Xu, Z. F., R. Mahmood, Z. L. Yang, C. B. Fu, and H. Su, 2015: Investigating diurnal and seasonal climatic response to land use and land cover change over monsoon Asia with the community earth system model. *J. Geophys. Res: Atmos.*, **120**, 1137−1152, https://doi.org/10.1002/2014JD022479.

Yang, X. C., Y. L. Zhang, L. S. Liu, W. Zhang, M. J. Ding, and Z. F. Wang, 2009: Sensitivity of surface air temperature change to land use/cover types in China. *Science in China Series D: Earth Sciences*, **52**(8), 1207−1215, https://doi.org/10.1007/s11430-009-0085-0.

Yang, X. C., Y. L. Zhang, M. J. Ding, L. S. Liu, Z. F. Wang, and D. W. Gao, 2010: Observational evidence of the impact of vegetation cover on surface air temperature change in China. *Chinese J. Geophys.*, **53**(4), 833−841, https://doi.org/10.3969/j.issn.0001-5733.2010.04.008. (in Chinese with English abstract)

Yuan, Y. F., and P. M. Zhai, 2022: Latest understanding of extreme weather and climate events under global warming and urbanization influences. *Transactions of Atmospheric Sciences*, **45**(2), 161−166, https://doi.org/10.13878/j.cnki.dqkxxb.20211011001. (in Chinese with English abstract)

Zhu, H. H., Y. Zhang, X. Y. Shen, S. Y. Wang, L. Y. Shang, and Y. Q. Su, 2018: A numerical simulation of the impact of vegetation evolution on the regional climate in the ecotone of agriculture and animal husbandry over China. *Plateau Meteorology*, **37**(3), 721−733, https://doi.org/10.7522/j.issn.1000-0534.2018.00050. (in Chinese with English abstract)